



## OPEN New design of a high-efficiency rectenna for wireless power transfer in 5G applications

Hamza Ben hamadi<sup>1</sup>, Said Ghnimi<sup>2</sup>, Mohamed Salah Karoui<sup>2,3</sup>, Ridha Ghayoula<sup>4</sup>, Nouredine Boulejfen<sup>2,5</sup>, Ali Gharsallah<sup>2</sup>, Amal Al-Rasheed<sup>6</sup> & Lotta Bayisenge<sup>7</sup>✉

This work presents a novel compact rectenna design for wireless power transfer (WPT) at 3.5 GHz, targeting 5G-enabled low-power IoT devices. The proposed system integrates an optimized patch antenna with a Schottky diode-based rectifier, enabling efficient RF-to-DC energy conversion in a compact footprint. A systematic co-design approach combining electromagnetic simulations and circuit-level modeling was employed to optimize impedance matching and maximize conversion efficiency. A parametric study of the load resistance revealed an optimal value of 5 k $\Omega$ , achieving peak power transfer efficiency under realistic operating conditions. The rectenna prototype was fabricated and experimentally characterized, confirming the simulation results and demonstrating a maximum DC output voltage of 0.91 V at an input power level of 0 dBm. The proposed design offers a practical, reproducible, and high-performance solution for 5G wireless energy harvesting, addressing the challenges of compactness, efficiency, and reliability for next-generation IoT applications.

**Keywords** Wireless Power Transfer (WPT), 5G, Rectenna, Schottky diode, Impedance matching, Internet of Things (IoT), RF-to-DC conversion

Wireless Power Transfer (WPT) is attracting increasing interest, particularly in the context of 5G networks and the Internet of Things (IoT), where the energy autonomy of connected devices is crucial. The 3.5 GHz band, frequently used in 5G NR (New Radio), represents a strategic opportunity for developing RF energy harvesting systems adapted to these new applications. Indeed, the rapid growth in the number of connected objects and the densification of 5G networks create an environment rich in electromagnetic energy in this band, which can be harvested and converted into useful energy through dedicated rectennas. Efficient energy harvesting in the 5G band requires an optimized design of the entire RF energy chain, from the antenna to the conversion circuit. The key role of the Schottky diode in this conversion process is well documented in the literature, thanks to its low forward voltage drop and fast switching speed, making it an essential component for WPT rectifiers. However, the efficiency of a rectenna is not uniform across all power levels. Diodes used in rectennas exhibit an optimal operating region in which they achieve maximum efficiency, typically corresponding to input power levels in the milliwatt-to-watt range<sup>1–30</sup>.

To address this challenge, Kim et al. introduced a radial power divider rectenna system that distributes a high incident power into multiple lower-power streams, thereby preserving the efficiency of Schottky diodes at higher power levels and ensuring system robustness in real environments with high signal density. This approach is particularly relevant for the 3.5 GHz band, where incident power can vary widely depending on the 5G network density<sup>1</sup>.

Impedance matching between the antenna and the rectifying diode plays a crucial role in achieving high RF-to-DC conversion efficiency. Dan et al. showed that the use of an integrated matching circuit combined with a harmonic suppression filter leads to a significant improvement in conversion efficiency at 2.45 GHz, a frequency range close to the 5G band investigated in this work. Their approach relies on a short-circuited microstrip line, which compensates for the capacitive behavior of the diodes while effectively suppressing unwanted harmonics,

<sup>1</sup>Universite Clermont Auvergne, EUPI, CNRS, Institut Pascal, Clermont-Ferrand F-63000, France. <sup>2</sup>Laboratory of Microwave Electronics, Faculty of Sciences of Tunis, University of Tunis El Manar, Tunis 2092, Tunisia. <sup>3</sup>Higher Institute of Applied Sciences and Technology of Mateur, University of Carthage, Carthage, Tunisia. <sup>4</sup>Department of Electrical and Computer Engineering, University of Waterloo, Waterloo, ON N2L 3G1, Canada. <sup>5</sup>Centre for Research on Microelectronics and Nanotechnology, Technopole of Sousse, Sousse 4050, Tunisia. <sup>6</sup>Department of Information Systems, College of Computer and Information Sciences, Princess Nourah bint Abdulrahman University, P.O. Box 84428, Riyadh, Saudi Arabia. <sup>7</sup>University of Rwanda, 4285 Kigali, Rwanda. ✉email: lotta.bayisenge@gmail.com

thereby enhancing DC output performance<sup>2</sup>. Such a technique can be readily extended to the 3.5 GHz band to maintain optimal energy conversion, even in the presence of diode nonlinearity.

The issue of polarization and angular coverage is also crucial for energy harvesting in mobile devices. Kumar et al. designed a multi-sector rectenna system that provides near-isotropic coverage, enabling effective energy harvesting even in cases of angular misalignment—a key factor for IoT devices operating in dynamic and variable environments<sup>3</sup>. Sood et al. extended this concept with a multi-element mirror structure that ensures almost omnidirectional 3D reception, particularly suited to the variability of 5G signals and the movement of connected objects<sup>4</sup>.

Bandwidth enhancement represents a key challenge for RF energy harvesting in the 5G spectrum, which typically extends over several hundred megahertz. Cao et al. introduced a wideband, multi-polarized rectenna architecture that integrates a hybrid coupler with a Class-F rectifier, enabling stable and high conversion efficiency across a wide frequency range and under different polarization conditions. This configuration is particularly well suited for energy harvesting in the 3.5 GHz band, where the transmitted signals may experience spectral dispersion due to the simultaneous operation of multiple 5G services<sup>5</sup>.

Miniaturization and compactness are essential requirements, particularly for IoT devices with embedded energy-harvesting capabilities. Lu et al. demonstrated that exploiting antisymmetric resonant modes allows a significant reduction in the physical size of Wi-Fi antennas without compromising radiation efficiency, offering clear advantages for the development of compact 5G antennas integrated into rectenna systems<sup>6</sup>. Furthermore, Liu et al. showed that direct integration of circuit components using a coplanar configuration with an embedded rectifying stage effectively minimizes insertion losses while enhancing the robustness and overall reliability of the harvesting system<sup>7,8</sup>.

The work by Ha et al. on spatially multiplexed traveling wave antennas provides an effective solution to ensure wide angular coverage ( $\pm 65^\circ$ ) while maintaining stable efficiency, a feature particularly suitable for energy harvesting in 5G scenarios where signal arrival angles vary significantly<sup>9</sup>. Similarly, advanced harmonic suppression approaches such as those by Moloudian and Dan are essential to stabilize the DC output voltage and reduce disturbances caused by diode nonlinearity, thereby ensuring optimal operation within the target band<sup>10,11</sup>. Shen et al.<sup>12</sup> proposed a compact duplexing rectenna capable of wireless power transfer (WPT) and harmonic feedback. It not only converts radio frequency (RF) power into direct current (DC) power at the fundamental frequency, but also feeds back the second harmonic signal from the power-limited receiver (Rx) to the transmitter (Tx), in order to stabilize the DC output when the dedicated power source is in motion. In<sup>13–18</sup>, the authors designed four dual-band and wideband rectennas for simultaneous wireless information and power transfer (SWIPT) are proposed. These approaches introduce an innovative concept in which conventional components are operated in reverse to provide additional functionality when combined with an antenna structure. In a similar vein, the studies reported in<sup>19–23</sup> investigate the potential of harvesting radio-frequency (RF) energy from existing wireless communication bands to supply power to low-consumption Internet of Things (IoT) devices. With the rapid expansion of IoT applications and wireless sensor networks (WSNs), the need for sustainable and autonomous energy solutions has become increasingly critical, particularly for extending device lifetime in remote or power-constrained environments where conventional energy sources are limited.

High-efficiency rectennas for Wireless Power Transfer (WPT) have been widely investigated due to their strong potential in emerging wireless applications; however, many reported design strategies continue to exhibit notable shortcomings. To strengthen the motivation of this study, the introduction presents a concise analysis of the main challenges that remain insufficiently addressed in current rectenna developments. These challenges include the degradation of RF-to-DC conversion efficiency at higher frequencies, particularly within the 5G spectrum, the difficulty of achieving wideband impedance matching, and the constraints associated with integration into compact Internet of Things (IoT) platforms. The proposed design is then discussed in relation to these issues, highlighting its enhanced conversion efficiency, reduced physical size, and relevance for 5G WPT scenarios. This discussion allows the contribution of the present work to be clearly positioned within the existing state of the art. Building on established design principles, an optimized rectenna operating at 3.5 GHz is developed, incorporating a dedicated impedance matching network for the rectifying diode and a low-pass filter to suppress harmonic components, thereby ensuring efficient and reliable wireless power transfer.

While numerous advanced rectenna configurations have been reported in the literature, many of these solutions depend on increased structural complexity, larger dimensions, or narrowly defined operating conditions. Despite their high reported performance, such architectures are often difficult to integrate into compact, low-cost, and easily deployable IoT receivers intended for operation in the 5G band.

Accordingly, the objective of this work is not to propose a radically new rectenna topology nor to rival highly sophisticated designs. Instead, the focus is placed on the development of a compact and experimentally validated rectenna operating at 3.5 GHz, based on a simple and reproducible methodology. The main contribution lies in the coherent co-design of the antenna and rectifier, the systematic optimization of the load conditions, and the experimental validation under realistic operating scenarios, with the goal of enabling practical wireless energy harvesting for low-power IoT devices.

The remainder of this paper is structured as follows: Sect. 2 outlines the methodological and conceptual framework, divided into three subsections addressing the fundamental operating principles, the development of the rectification circuits, and the design of the antenna respectively. Section 3 is dedicated to the analysis and discussion of the obtained results. Finally, Sect. 4 concludes the paper and highlights directions for future research.

## Principle and design method

### Principle

This work aims to design a rectenna operating at 3.5 GHz, intended for wireless power transfer (WPT) in the 5G band. The system is based on the direct conversion of incident RF energy into usable DC power, through the combination of a patch antenna and a Schottky diode rectifier circuit. The electromagnetic modeling of the antenna is performed using CST Studio Suite software, allowing the optimization of its structure for an input impedance of 50  $\Omega$ , good matching ( $S_{11} < -10$  dB), and efficient radiation at the target frequency. Once the antenna is validated, its S-parameters are extracted and imported into ADS (Advanced Design System) software for the rectifier circuit modeling, as shown in Fig. 1. This circuit integrates a Schottky diode characterized by a complex impedance:

$$Z_D = R_D + jX_D \quad (1)$$

A conjugate matching circuit is used to maximize power transfer according to the condition:

$$Z_{ant} = Z_D^* \quad (2)$$

And a low-pass filter to block the harmonics generated during the RF-DC conversion, while allowing the useful DC component to pass through.

The overall efficiency directly depends on the quality of the impedance matching and harmonic suppression; therefore, a filter is also designed as a short-circuited quarter-wave transmission line, exhibiting a reactive impedance

$$Z_{HF} = jX_{HF} \quad (3)$$

To compensate for the imaginary part of the diode impedance at the fundamental frequency. The antenna's input impedance is thus adjusted to satisfy the relation:

$$Z_{ant} = R_{ant} + jX_{ant} = (Z_D + Z_{HF})^* \quad (4)$$

Assuring a high rectification efficiency. This modular approach, separating electromagnetic design (in CST) and circuit design (in ADS), enables a comprehensive optimization of the system for efficient wireless power transfer, intended to supply low-power devices such as IoT sensors.

### Rectification circuits design

The Skyworks SMS7630-079LF Schottky diode is used as the main rectifying element in this study. It is specifically designed for RF applications due to its favorable characteristics: low series resistance ( $R_s = 20$   $\Omega$ ), very low junction capacitance ( $C_j = 0.14$  pF), and low threshold voltage (approximately 240 mV). These properties enable efficient conversion of the RF signal into DC voltage at high frequencies, particularly at 3.5 GHz.

The impedance of this diode at high frequency can be estimated using the following formula<sup>2</sup>:

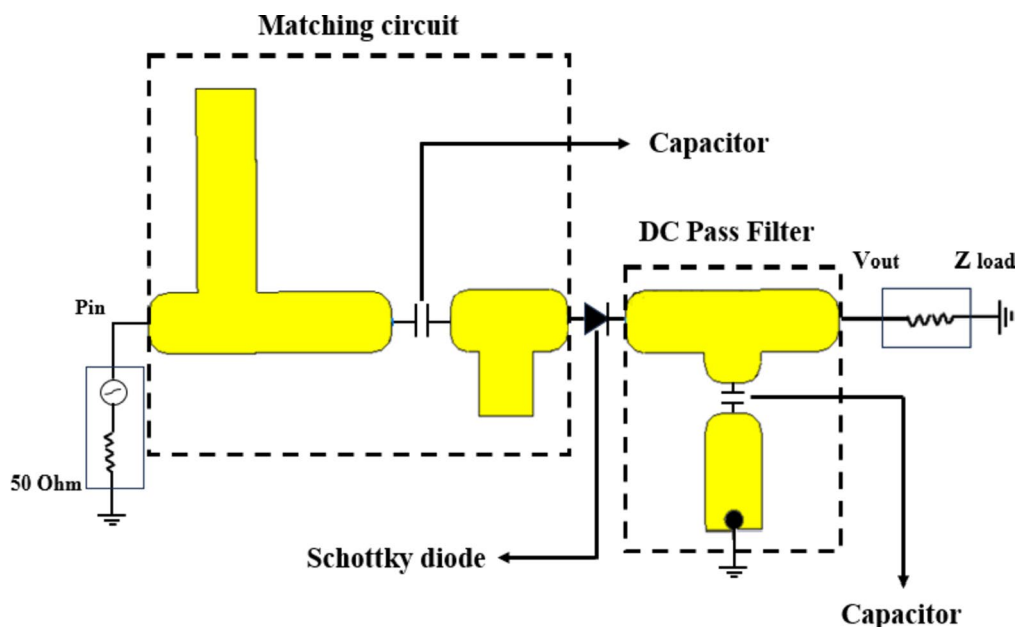


**Fig. 1.** Configuration of the compact reconfigurable rectenna.

$$Z_D = \frac{\pi R_s}{\cos(\theta_{0n}) \left( \frac{\theta_{0n}}{\cos(\theta_{0n})} - \sin(\theta_{0n}) \right) + j\omega R_s C_j \left( \frac{\pi - \theta_{0n}}{\cos(\theta_{0n})} + \sin(\theta_{0n}) \right)} \tag{5}$$

However, as a simplified approximation for an initial design, the following model can be used:

$$Z_D = R_D + \frac{1}{j\omega C_j} \tag{6}$$

It should be noted that this simplified impedance expression is used solely for indicative purposes and for an initial estimation. The final impedance matching network is subsequently optimized through nonlinear harmonic-balance simulations in ADS, based on the manufacturer-provided Schottky diode model, which inherently accounts for the diode's nonlinear behavior and parasitic effects.

At 3.5 GHz, the angular frequency is  $\omega = 2\pi f = 2,199 \times 10^{10}$  rad/s, which gives a capacitive reactance of:

$$X_c = \frac{1}{\omega C_j} = \frac{1}{2,199 * 10^{10} * 0,14 * 10^{-12}} \approx 353\Omega \tag{7}$$

Hence, the estimated complex impedance of the diode is:

$$Z_D \approx 20 - j353 \tag{8}$$

Based on a small-signal estimation of the Schottky diode impedance at 3.5 GHz, an initial impedance matching network was designed using Advanced Design System (ADS). This preliminary analysis serves as a starting point for the rectifier design. In practice, due to the nonlinear behavior of the rectifying diode and the strong dependence of the rectifier input impedance on both the DC load resistance and the incident RF power level, the matching network was further optimized using nonlinear harmonic-balance simulations. The optimization was carried out under realistic operating conditions, considering high-resistance DC loads. Unless otherwise stated, a load resistance of 5 kΩ (identified as the optimal value through the parametric study presented in Fig. 13) was used as the reference load. Figure 2 shows the complete microstrip implementation of the rectifier circuit, and the highlighted loop indicates the DC return path: the rectified DC current flows from the output node through the load and returns to the diode via the common ground plane, thereby closing the DC loop<sup>13</sup>.

Figure 2 illustrates the complete schematic of the rectifier simulated in the ADS environment, including the diode, the matching network, and the output filter. Based on this schematic, Fig. 3 illustrates  $S_{11}$  evaluated using Harmonic Balance combined with Large-Signal S-Parameter (HB-LSSP) analysis at an input power level of  $P_{in} = 0$  dBm. A minimum value of approximately -33 dB is observed near 3.5 GHz, indicating very good impedance matching of the rectifier under this nonlinear operating condition.

The analysis of the simulated input impedance  $Z_{IN}$  at the anode terminal of the diode, shown in Fig. 4, reveals a real part close to 50 Ω and a nearly zero imaginary component at 3.5 GHz. This condition indicates an ideal impedance match between the antenna and the diode anode, ensuring maximum power transfer. The absence of residual reactance at this frequency confirms the circuit's performance in terms of matching and RF-to-DC conversion efficiency, a key requirement for wireless power transfer systems.

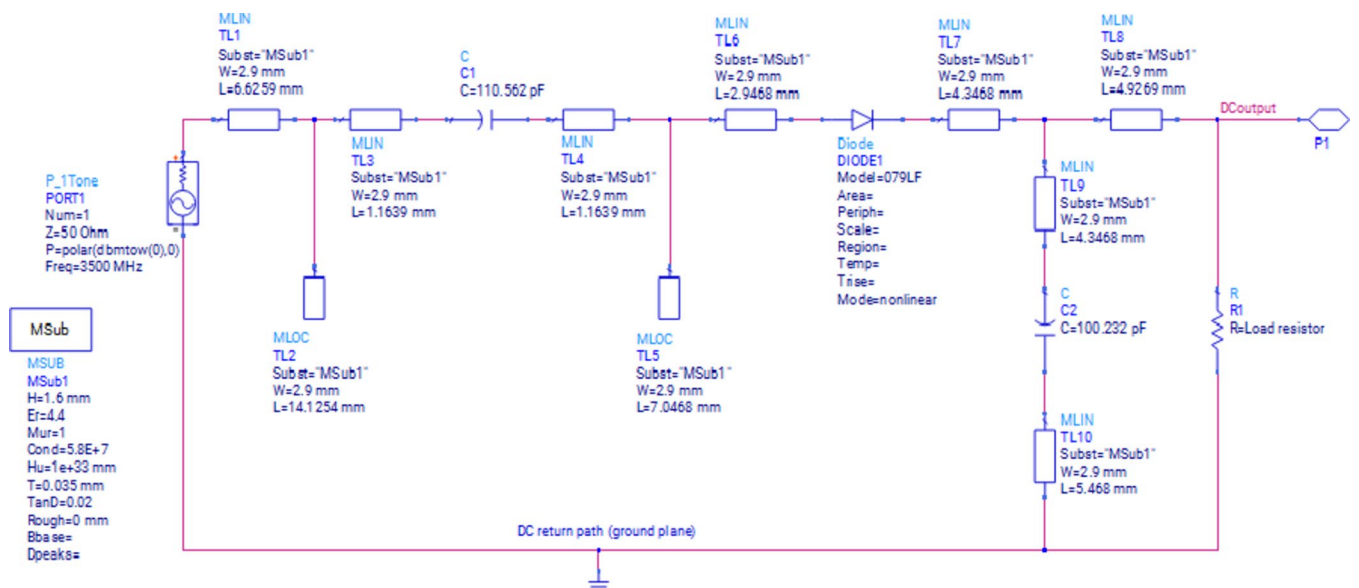


Fig. 2. ADS schematic of the rectifier circuit with a 5 kΩ output load.

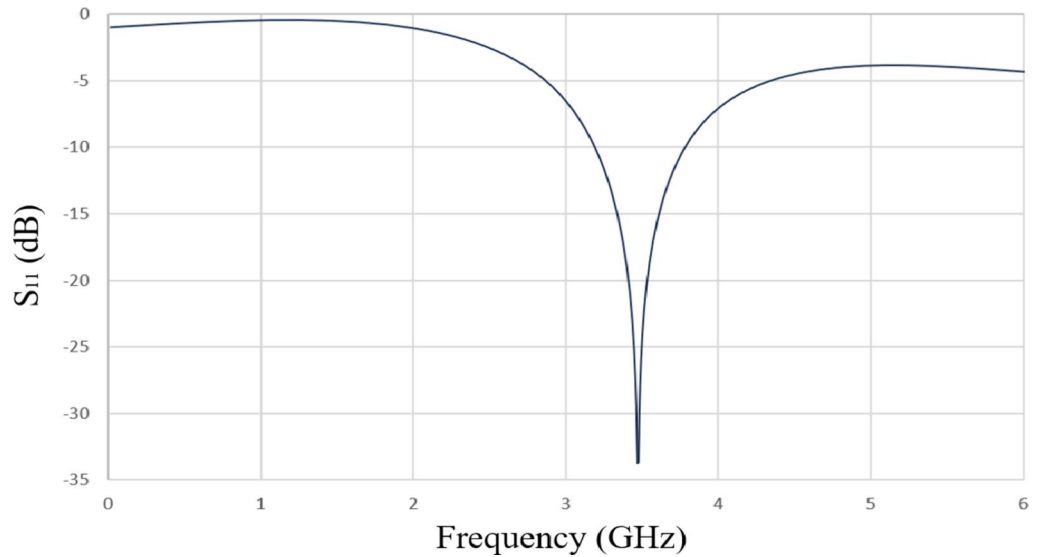


Fig. 3. Simulated reflection coefficient of the rectifier.

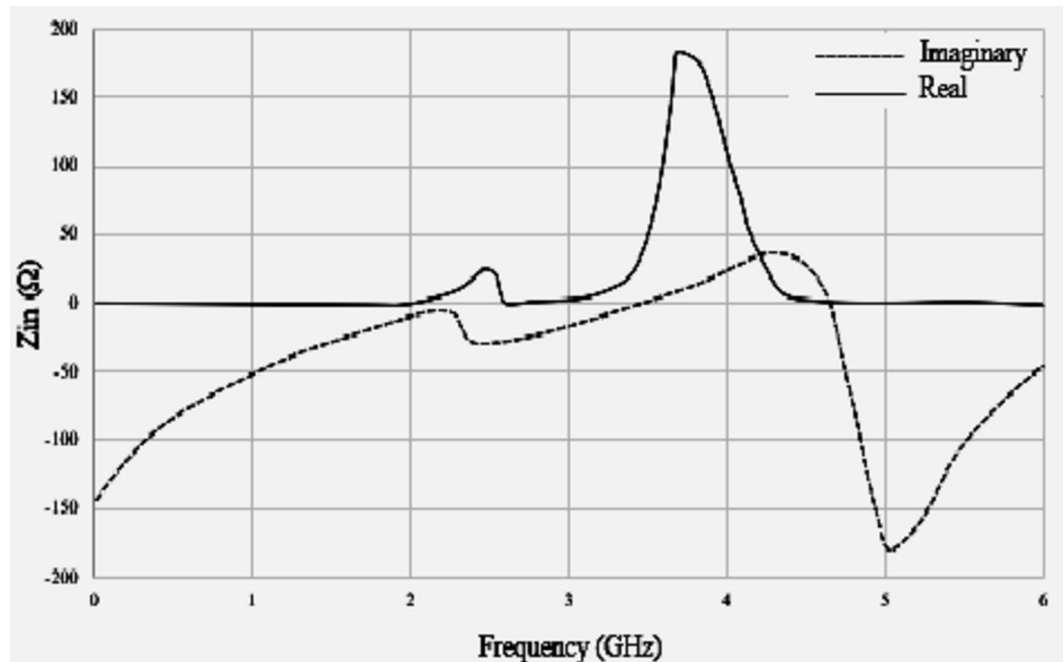
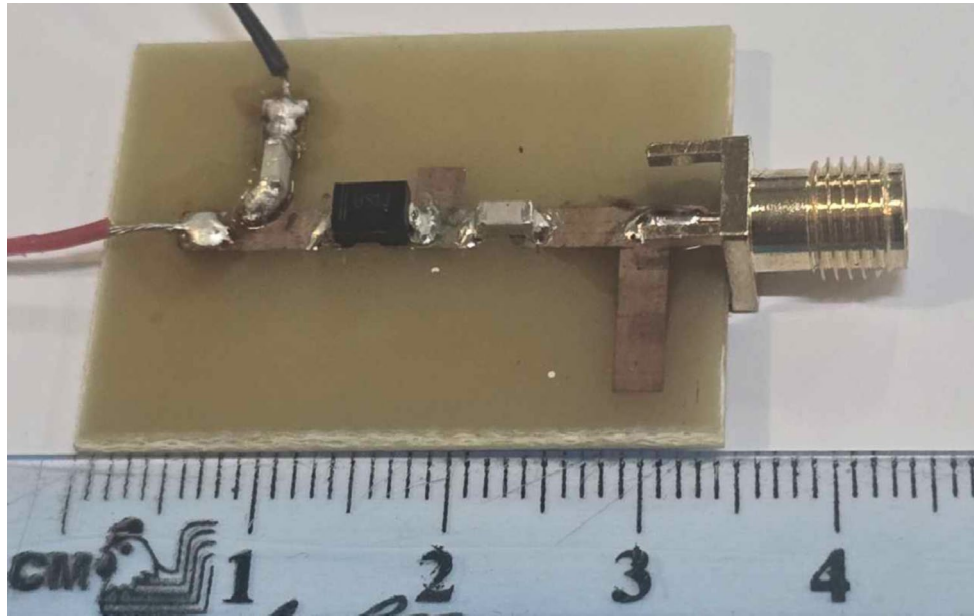


Fig. 4. Simulated antenna input impedance as a function of frequency.

Finally, Fig. 5 shows the fabricated rectenna prototype. The printed circuit board is clearly visible, along with carefully dimensioned microstrip lines, surface-mounted components (SMD), and the RF input port. This implementation closely mirrors the simulated circuit and validates the consistency between theoretical design and practical fabrication.

#### 5G-oriented patch antenna topology

In wireless power transfer (WPT) applications, the receiving antenna must meet specific requirements that differ from those of conventional communication antennas. Beyond bandwidth considerations, a WPT receiving antenna must ensure stable impedance behavior around the target frequency, efficient energy harvesting under low incident power levels, compact dimensions, and compatibility with rectifier integration. In rectenna-based systems, the interaction between the antenna and the nonlinear rectifying circuit plays a critical role in determining the overall RF-to-DC conversion efficiency. Consequently, the objective of the proposed antenna



**Fig. 5.** Fabricated rectenna prototype

design is not limited to bandwidth enhancement but also aims to provide a suitable impedance environment to enable efficient power transfer to the rectifier.

The proposed antenna design was developed in a step-by-step manner, as illustrated in Fig. 6. It begins with a basic structure consisting of a rectangular microstrip patch antenna fed by a microstrip line and printed on an FR-4 substrate with a thickness of 1.58 mm, a relative permittivity of 4.4, and a moderate loss tangent. This initial configuration exhibits a very narrow bandwidth centered around 3 GHz, which is significantly offset from the target frequency of 3.5 GHz intended for 5G applications.

The choice of the FR-4 substrate is motivated not only by its low cost, wide availability, and ease of fabrication, but also by its relevance for compact RF devices intended for industrial applications. Although FR-4 exhibits a higher loss tangent compared to dedicated RF substrates, it remains widely employed in RF energy harvesting systems and low-cost rectenna designs, where a balanced trade-off between electromagnetic performance, system integration, and technological feasibility is required. This material choice enables rapid prototyping, realistic experimental validation, and improved suitability for practical wireless power transfer (WPT) applications.

To shift the antenna resonance toward the target operating frequency, a rectangular slot is etched at the center of the patch. This modification extends the effective electrical path of the surface currents, causing a reduction in the resonant frequency toward 3.5 GHz while maintaining a compact antenna footprint. Nevertheless, this adjustment primarily influences the resonance position and does not provide a substantial improvement in impedance bandwidth. To achieve more stable impedance matching and ensure reliable operation when coupled with the rectifier, an additional radiating element with a diamond-shaped geometry is placed above the initial patch. This geometry introduces a progressive variation in current path length and supports a more homogeneous surface current distribution than conventional rectangular shapes, leading to smoother impedance characteristics and improved radiation stability. The diamond-shaped element is linked to the main patch through two curved microstrip lines. These curved connections are designed to minimize abrupt impedance transitions and reduce current concentration, allowing a smoother electromagnetic field transition and stronger coupling between the radiating elements. Consequently, the antenna exhibits improved impedance matching over an extended frequency range, which is particularly advantageous for rectenna applications.

Finally, supplementary slots are introduced into the diamond-shaped element to further adjust the impedance matching and suppress undesired higher-order resonant modes. This carefully controlled geometric refinement enables accurate tuning of the effective electrical length and coupling mechanism, resulting in a compact antenna operating at 3.5 GHz with enhanced impedance bandwidth and improved matching performance (Fig. 7).

These characteristics contribute to stable energy reception and efficient rectifier operation in wireless power transfer applications.

For better visualization, the antenna dimensions are summarized in the Table 1.

Figure 8 shows the evolution of the reflection coefficient  $S_{11}$  throughout the antenna design process. The different curves illustrate the progressive impact of the geometric modifications made to the structure. At each stage, the adjustments contributed to improved impedance matching and bandwidth enhancement, while gradually shifting the resonance frequency toward the target value of 3.5 GHz.

The final antenna structure achieves an impedance bandwidth defined by  $|S_{11}| < -10$  dB from 3.32 GHz to 3.94 GHz around the target frequency of 3.5 GHz, which corresponds to a  $-10$  dB fractional bandwidth of approximately 11.4% and confirms the effectiveness of the proposed design in enhancing impedance bandwidth.

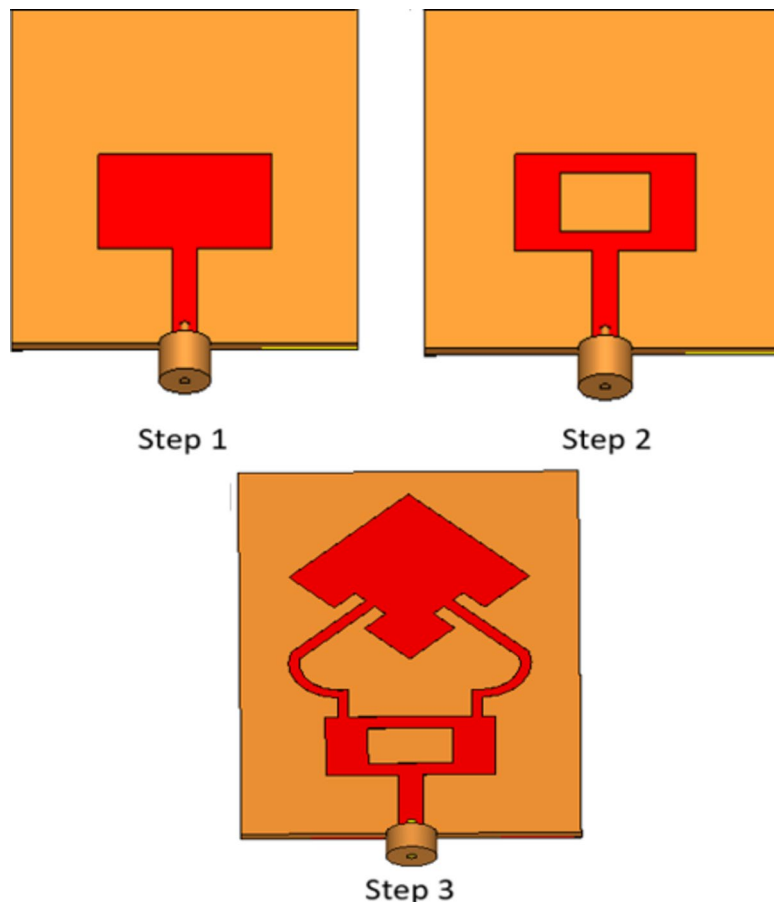


**Fig. 6.** Evolution of the Antenna Structure.

To validate the performance of the designed structure, a prototype of the final antenna was fabricated and experimentally characterized. The reflection coefficient was measured using a vector network analyzer. The experimental results show a slight frequency shift compared to the simulated curves, generally toward slightly higher frequencies. This discrepancy can be attributed to several sources of error, including fabrication tolerances, dielectric dispersion, losses introduced by coaxial cables and connectors, as well as inaccuracies related to soldering and the measurement environment.

Despite these deviations, the measured curve remains largely consistent with the simulation, thereby confirming the validity of the proposed model and the reliability of the design (Figure 9). The fabricated antenna prototype used for the experimental characterization is shown in Fig. 9(b), and the measured  $|S_{11}|$  remains below  $-10$  dB around 3.5 GHz, confirming suitable impedance matching for rectenna operation.

The simulated and experimental radiation patterns are presented in the E- and H-planes to evaluate the directional behavior of the antenna (Fig. 10). A strong correlation is observed between the numerical simulations and the measurement results. The H-plane exhibits a quasi-omnidirectional radiation pattern, which is particularly suitable for mobile communication applications. In contrast, the E-plane shows a moderate level of directivity that remains in line with the expected antenna behavior. The measured antenna gain is close to 5 dB, in good agreement with the simulated results, thereby validating the antenna's radiation efficiency.

Overall, these findings confirm that the proposed antenna structure is not only properly matched in terms of operating frequency but also satisfies the radiation performance requirements for 5G communication systems.

## Results and discussion

The rectenna consists of the antenna modeled in the previous section, coupled with a rectifier circuit based on a Schottky diode SMS7630-079LF, a microstrip matching network, and a low-pass filter designed to isolate the DC component at the rectifier output while suppressing higher-order RF harmonics generated by the nonlinear behavior of the rectifying diode. The output of the rectifier is connected to a resistive load and the resulting DC voltage is measured using a digital voltmeter.

This configuration allows the evaluation of the RF–DC conversion performance of the system under conditions close to a real environment, while ensuring optimal impedance matching through the precise design of both the antenna and the rectifier (Fig. 11).

The measurement setup was implemented in an anechoic chamber to eliminate unwanted electromagnetic reflections. A linearly polarized horn antenna, fed by a fixed-frequency RF signal generator operating at

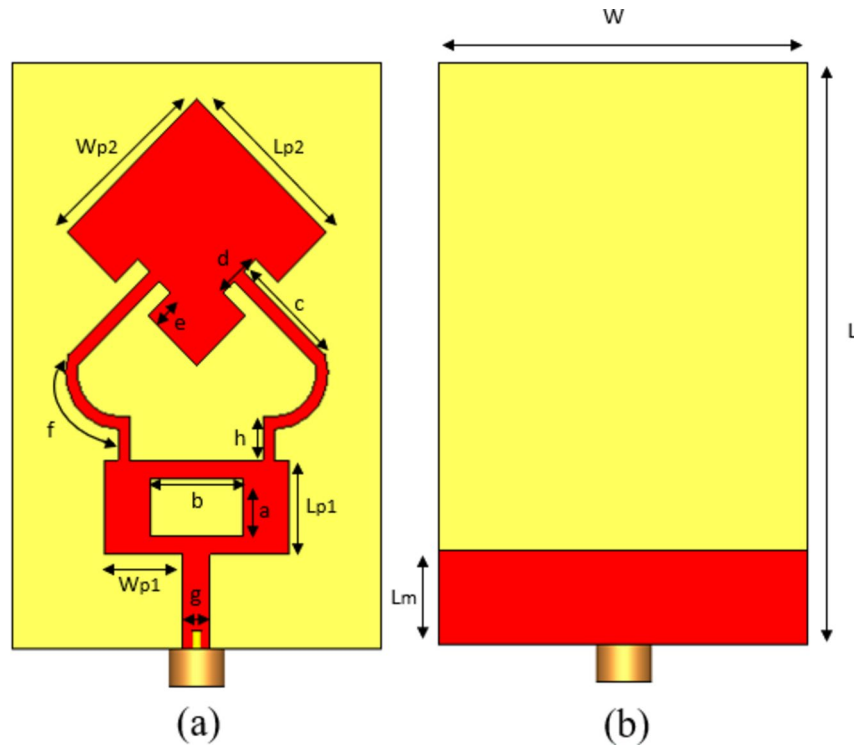


Fig. 7. Proposed 5G antenna configuration.

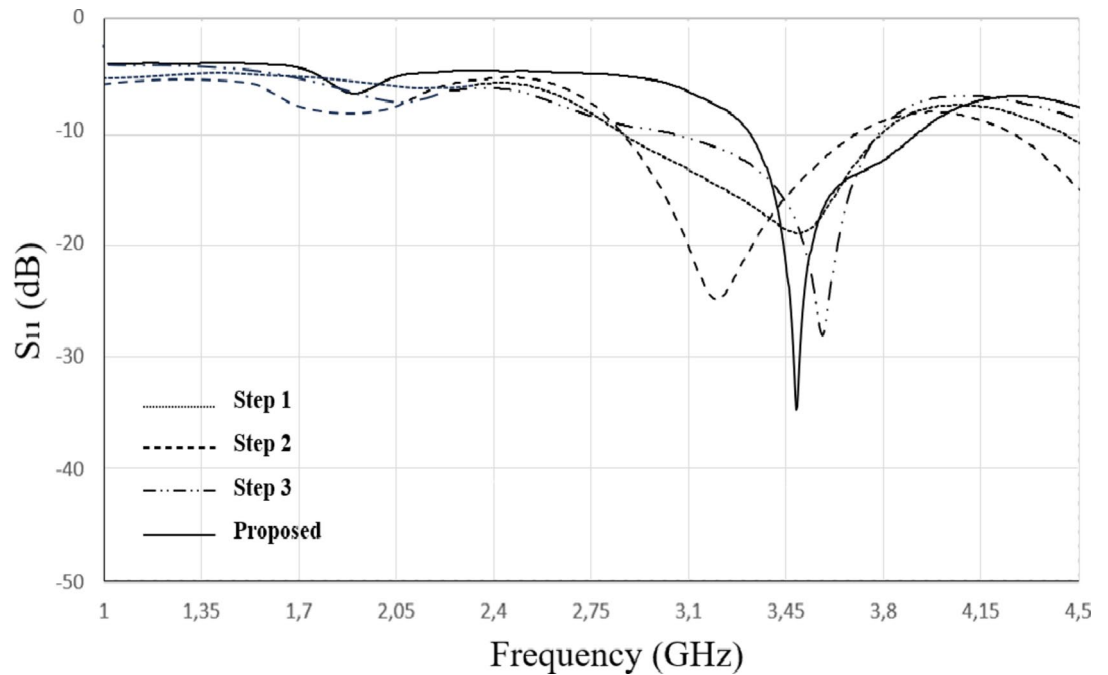
Parameters	Values (mm)
L	57.5
W	40
Lm	10
Lp1	10
Lp2	14.5
Wp1	8.52
Wp2	15
a	6
b	10
c	8.85
d	3.53
e	2.47
f	5.45
g	2.94
h	4.6

Table 1. Geometric parameters of the antenna.

3.5 GHz, served as the transmitting source and was directed toward the rectenna under test. The polarization of the horn antenna was carefully aligned with that of the rectenna in order to maximize the received power and minimize polarization mismatch losses. The transmitting horn antenna provides a nominal gain of  $G_{TX} = 10$  dBi at 3.5 GHz, according to the manufacturer’s specifications.

After the modeling and experimental implementation of the rectenna, including wiring and device calibration, a load resistor ( $R_L$ ) was added at the output of the low-pass filter. This configuration allows evaluation of the impact of  $R_L$  on the obtained DC voltage as well as on the power conversion efficiency (Fig. 12). A parametric study was conducted by varying this resistance, highlighting its direct influence on the overall performance of the wireless power transfer system.

The selected load resistance range (3–9 k $\Omega$ ) corresponds to the typical input impedances of ultra-low-power IoT devices and energy management circuits operating in the sub-milliwatt regime. This range also provides an



**Fig. 8.** Evolution of the reflection coefficient  $S_{11}$ .

optimal trade-off between output voltage increase and delivered current, which is essential for achieving high rectifier efficiency at low input power levels.

This configuration provides a controlled framework for evaluating the RF–DC conversion behavior of the rectenna while enabling a systematic investigation of the influence of the load resistance on the delivered DC power.

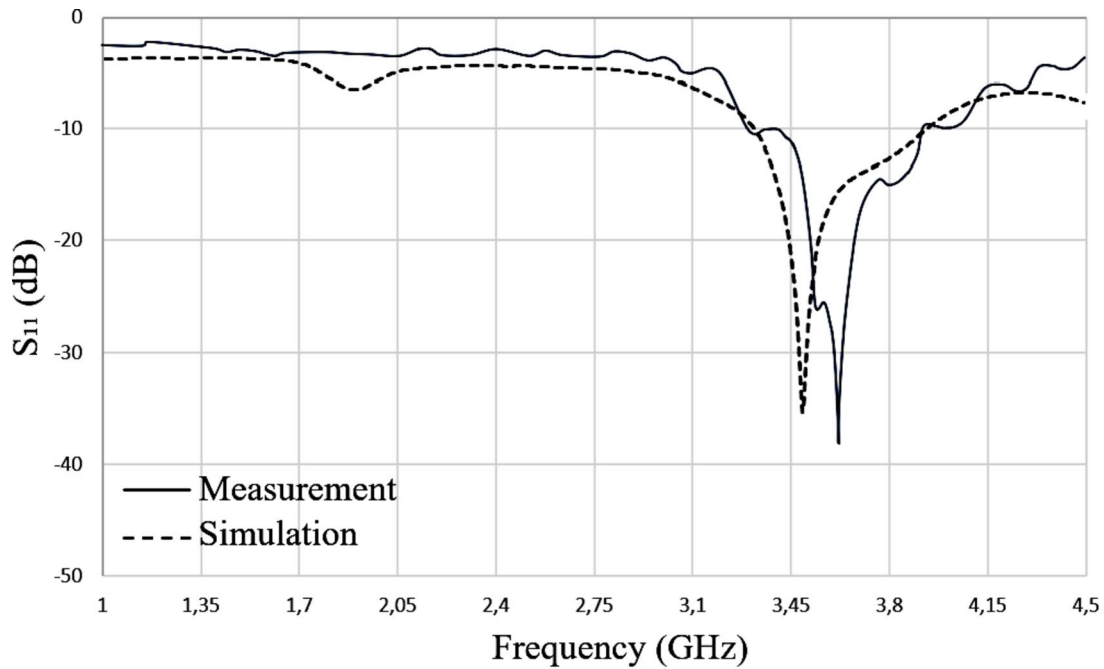
A parametric study was conducted by varying  $R_L$  over four representative values (3, 5, 7, and 9 k $\Omega$ ) across a wide range of incident RF power levels. The results demonstrate that the load resistance plays a critical role in determining both the output voltage and the RF–DC power conversion efficiency. As shown in Fig. 13, the conversion efficiency increases with input power and reaches its maximum when  $R_L = 5$  k $\Omega$  for input power levels above  $-15$  dBm, indicating an optimal impedance matching condition between the rectifier and the load.

At lower input power levels, particularly below  $-15$  dBm, lower resistance values such as 3 k $\Omega$  and 5 k $\Omega$  yield slightly higher output voltages due to more effective charge accumulation at the rectifier output. However, when considering the entire investigated power range,  $R_L = 5$  k $\Omega$  consistently provides the most favorable trade-off between delivered current and output voltage, leading to the highest overall RF–DC conversion efficiency. These results highlight the importance of proper load selection for achieving efficient rectenna operation, especially in low-power wireless energy harvesting applications.

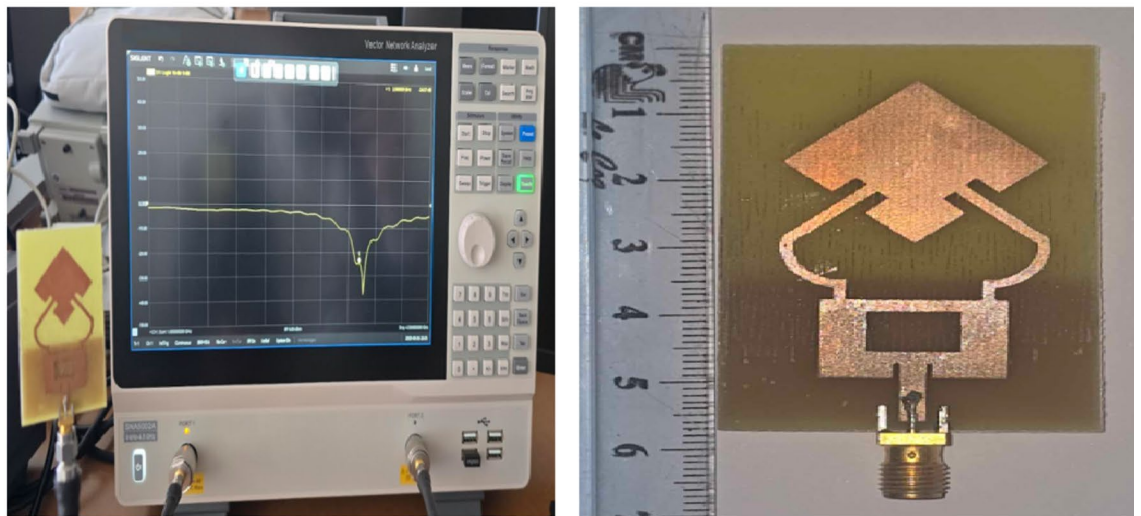
Figure 14 illustrates the evolution of the output voltage as a function of the input power for a load resistance of  $R_L = 5$  k $\Omega$ , selected based on previous simulation results. The simulated data exhibit an overall quasi-linear behavior, with the output voltage increasing progressively as the input power rises. A maximum output voltage of 1.46 V is reached at 0 dBm, thereby confirming the effectiveness of the system under ideal conditions.

In contrast, the experimental measurements show a lower maximum output voltage of approximately 0.91 V at 0 dBm. Furthermore, the measured curve does not strictly follow the linear trend observed in the simulations. This discrepancy can be attributed to several practical factors, including printed circuit board fabrication tolerances and inaccuracies related to manual soldering. Additionally, the nonlinear behavior of the Schottky diode under high excitation levels, parasitic effects associated with the diode package and solder pads, losses introduced by the FR-4 substrate and the microstrip transmission lines, as well as connection and measurement losses, all contribute to the observed reduction in the measured output voltage. Such differences between simulated and experimental results are commonly reported in RF rectifier implementations and do not compromise the overall validity of the observed performance trends.

To further assess the frequency sensitivity of the rectifier, the RF-to-DC conversion efficiency was evaluated as a function of frequency across the 5G band. This analysis was performed under realistic operating conditions using a fixed load resistance of  $R_L = 5$  k $\Omega$  and two representative input power levels ( $P_{in} = -10$  dBm and  $P_{in} = 0$  dBm). The results show that the rectifier maintains a relatively stable efficiency around the design frequency of 3.5 GHz, with a gradual degradation toward the band edges (see in Fig. 15). This behavior is mainly governed by the frequency-dependent impedance matching between the antenna and the rectifier, as well as by the nonlinear characteristics of the Schottky diode and the low-pass filtering stage. These findings confirm that the proposed rectifier is well suited for wireless power transfer applications within the targeted 5G sub-6 GHz band.



(a)



(b)

**Fig. 9.** (a) Comparison of Simulated and Measured S11 (b) Antenna Prototype.

Table 2 compares the proposed rectenna with several recent designs operating at or close to the 3.5 GHz range. It should be emphasized that only a limited number of rectenna studies specifically address the 3.5 GHz band dedicated to 5G systems, whereas many reported works focus on neighboring frequency bands typically related to 4G or ISM applications. A number of these designs obtain high RF–DC conversion efficiencies by employing low-loss substrates such as Rogers or RT Duroid and by operating at relatively high input power levels, generally above 0 dBm. In contrast, rectennas designed for cost-sensitive or sustainable IoT applications often rely on FR-4 substrates, valued for their low cost and wide industrial availability. This choice simplifies fabrication and supports practical deployment, although it typically results in more moderate conversion performance. Therefore, judging performance solely on the basis of efficiency can be misleading, as this parameter is closely linked to both the input power level and the operating frequency. To ensure a more balanced and meaningful evaluation of the different designs, the power/frequency-weighted efficiency (PFE) metric proposed in<sup>24</sup> is employed as a unified performance criterion, expressed as

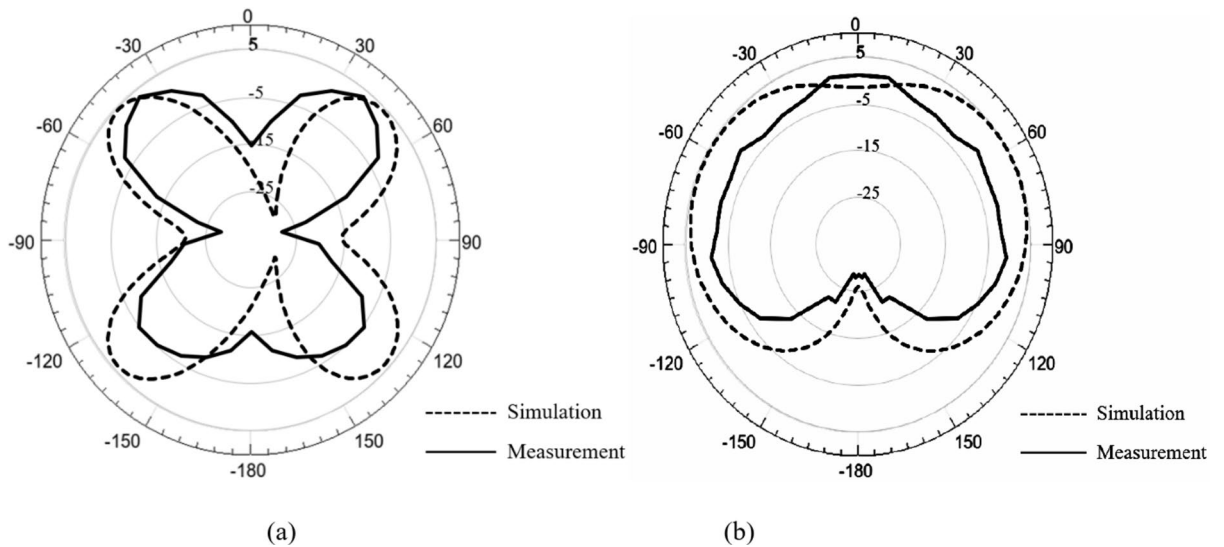


**Fig. 10.** Simulated and Measured Radiation Patterns in (a) E Plane and (b) H Plane.

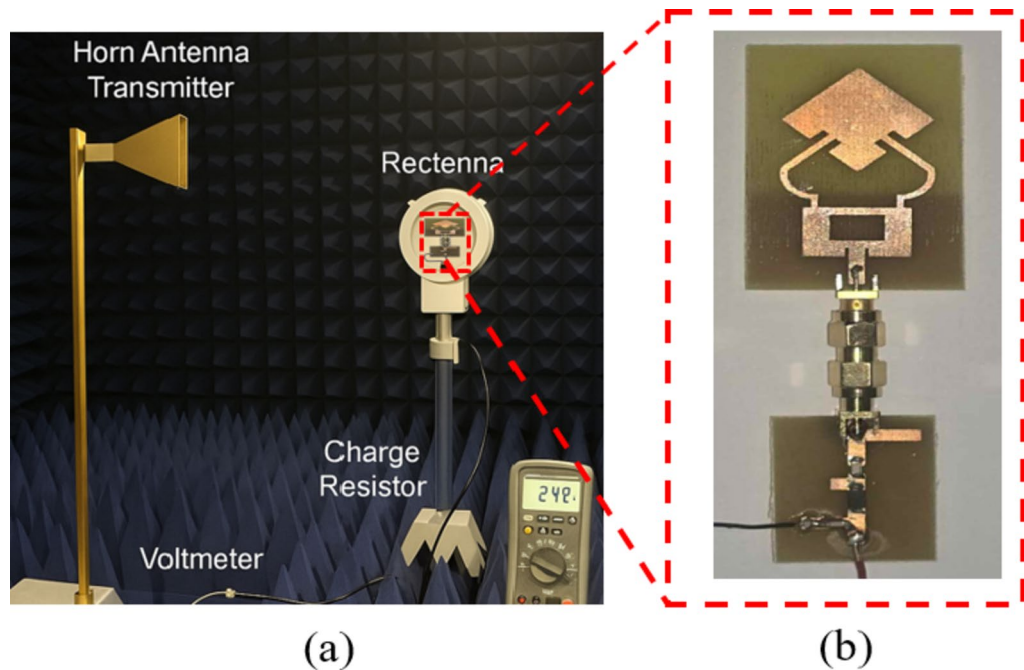


**Fig. 11.** (a) Rectenna Measurement Setup (b) Rectenna Prototype.

$$PFE = \frac{1}{m} \sum_{j=1}^m \sum_{i=1}^n \eta_{ij} f_i^{0.25} P_j^{-0.1} \tag{9}$$

where  $\eta_{ij}$  denotes the RF–DC conversion efficiency,  $f_i$  is the operating frequency in GHz, and  $P_j$  is the input power in mW.

In comparison with the reported designs, the proposed rectenna is positioned around a deployment-driven objective rather than peak efficiency under optimized laboratory conditions. Several high-efficiency implementations in Table 2 benefit from low-loss substrates and characterization at relatively favorable input power levels, which can inflate the apparent performance for scenarios where ambient RF levels are limited. The present work instead emphasizes practicality: a compact realization on low-cost FR-4 and evaluation at 0 dBm to reflect operating conditions that are more representative of scalable IoT energy-harvesting nodes. While this choice inherently constrains the maximum achievable RF–DC efficiency relative to premium-substrate

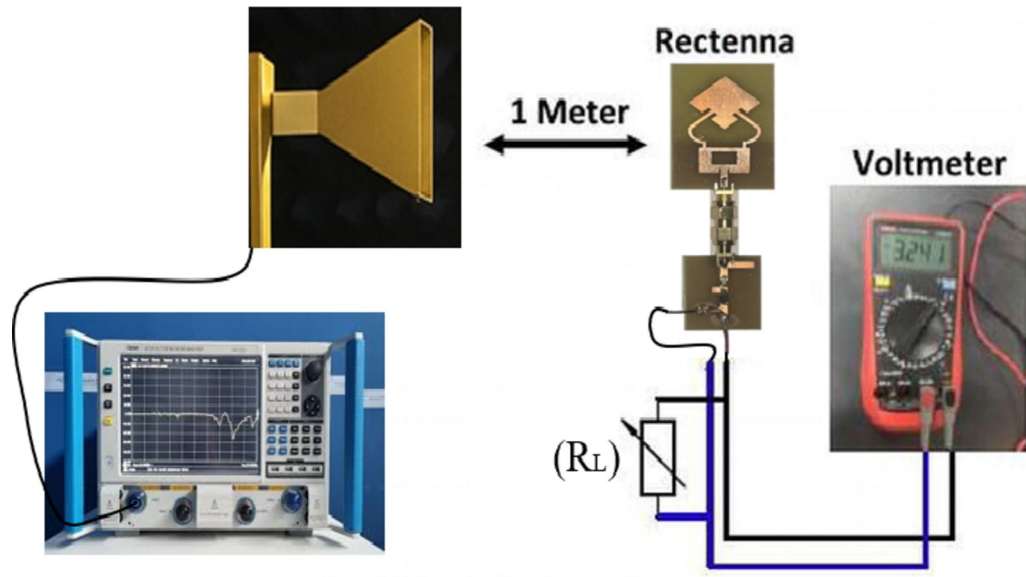


Fig. 12. Overall System Configuration.

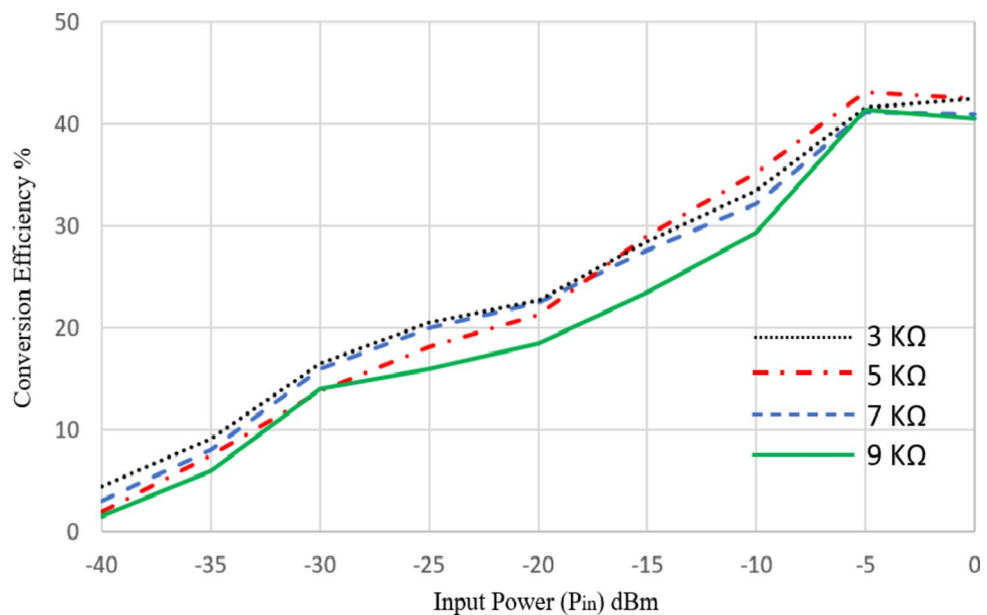


Fig. 13. Frequency-dependent RF-to-DC power conversion efficiency of the proposed rectifier.

solutions, it improves manufacturability and reproducibility and yields a conversion performance that remains meaningful in realistic regimes. The PFE-based comparison further supports this viewpoint by reducing the bias introduced by frequency and input power, thereby highlighting the proposed design as a balanced trade-off between cost, simplicity, and usable energy conversion.

**Conclusion**

This work has presented the design, simulation, and experimental validation of a compact wireless power transfer system intended for 5G applications operating in the 3.5 GHz band. The proposed architecture is based on a rectenna combining a microstrip patch antenna with a rectifying circuit employing a Schottky diode (SMS7630-079LF).

Antenna characterization results indicate adequate impedance matching at the target frequency, with a reflection coefficient below -10 dB, along with a stable radiation pattern and a gain level consistent with the requirements of IoT devices. The rectifying circuit, designed and optimized using ADS, provides a stable DC

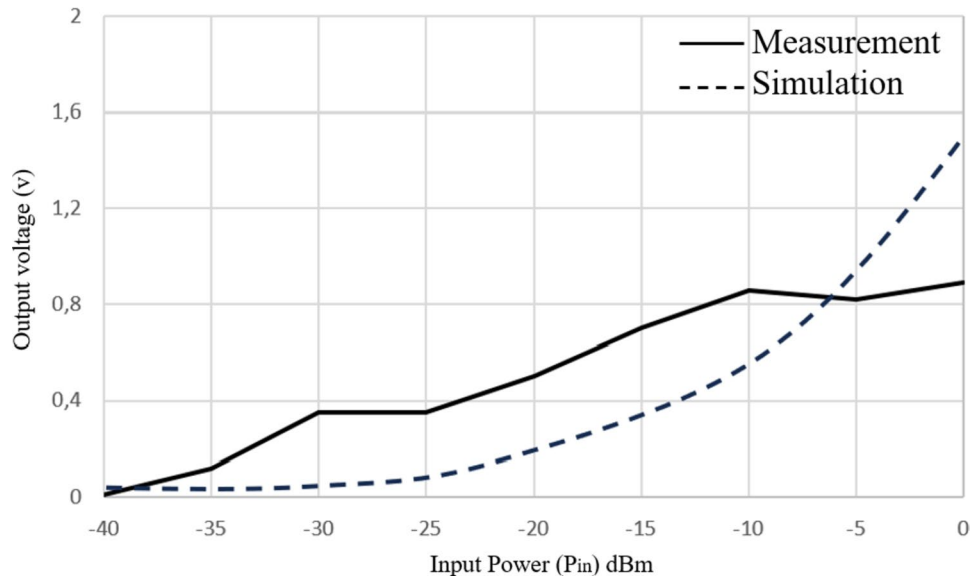


Fig. 14. Output Voltage vs. Input Power at  $R_L = 5\text{ k}\Omega$ .

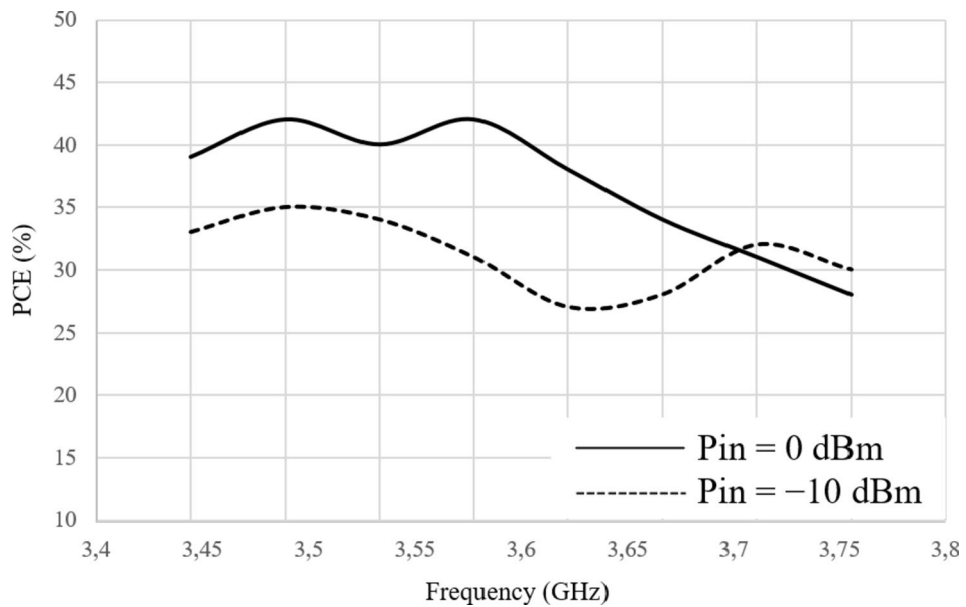


Fig. 15. Frequency-dependent RF-to-DC power conversion efficiency of the proposed rectifier.

Ref.	Frequency (GHz)	Substrate	Rectenna Size	Peak RF–DC Efficiency	Input Power Level	PFE	Remarks
<sup>25</sup>	3.5	Fr-4	Compact	58%	5 dBm	70.6	Reconfigurable beam, 5G band
<sup>26</sup>	2.45 / 3.6	Rogers	Compact	59% / 41%	2 dBm	124.4	Ambient RF harvesting
<sup>27</sup>	2–18	Rogers	Compact / Planar PCB	40%	-5 dBm	56.2	Wilkinson split/ Dual-pol, wideband
<sup>28</sup>	0.9–5.8	CMOS (on-chip)	IC-level	Up to 60%	-20 to 0 dBm	120.34	FoM-based comparison
<sup>29</sup>	3.3–3.6 4.8–5.0	Rogers	Compact	67.6%	5 dBm	157.72	Dual-band sub-6 GHz rectifier
<sup>30</sup>	3.5	Alumina + FR-4	Compact	67.16%	5 dBm	81.87	CP RDRA + single shunt diode rectifier
This work	3.5	FR-4	Compact	42%	0 dBm	57.45	Low-cost, ambient RF harvesting

Table 2. Performance Comparison of 3.5 GHz Rectennas for RF Energy Harvesting Applications.

output voltage through the implementation of an appropriate impedance matching network and a low-pass filter. A parametric analysis of the load resistance shows that an optimal RF-to-DC conversion efficiency is achieved for a load value of 5 k $\Omega$  at an input power level of -15 dBm, which is representative of ambient RF energy harvesting conditions. Experimental measurements generally follow the simulated trends, with minor discrepancies attributed to fabrication tolerances and measurement uncertainties.

These results confirm the feasibility of a compact rectenna operating in the 3.5 GHz 5G band for low-power IoT applications. However, the efficiency degradation observed at very low input power levels remains a limitation that must be addressed. Future work will focus on further optimization of the rectifying circuit, investigation of the system behavior under different RF illumination conditions, and extension of the proposed approach to more complex deployment scenarios.

## Data availability

The datasets used during the current study are available from the corresponding author on reasonable request.

Received: 6 November 2025; Accepted: 5 March 2026

Published online: 08 March 2026

## References

- Kim, D. H., Oh, S. Y., Park, H. S. & Hong, S. K. A power dividing rectenna system for high-power wireless power transfer for 2.45-GHz band. *IEEE Access*. **12**, 1–9. <https://doi.org/10.1109/ACCESS.2024.3416169> (2024).
- Dan, Z., He, Z., Lin, H. & Liu, C. A patch rectenna with an integrated impedance matching network and a harmonic recycling filter. *IEEE Antennas Wirel. Propag. Lett.* **21** (10), 2085–2089. <https://doi.org/10.1109/LAWP.2022.3190879> (2022).
- Kumar, S., Kumar, M. & Sharma, A. A compact stacked multisector near-isotropic coverage rectenna array system for IoT applications. *IEEE Microw. Wirel. Technol. Lett.* **34** (1), 123–126. <https://doi.org/10.1109/LMWT.2023.3331214> (2024).
- Sood, D., Kumar, M. & Ubhi, J. S. A DC combining-free miniaturized mirror-like rectenna system with full-wave rectification for robust wireless power transfer in IoT at 2.45 GHz. *IEEE Microw. Wirel. Technol. Lett.* **35** (4), 448–451. <https://doi.org/10.1109/LMWT.2025.3538629> (2025).
- Cao, C., Zhang, X., Song, C., Georgiadis, A. & Goussetis, G. A highly integrated multipolarization wideband rectenna for simultaneous wireless information and power transfer (SWIPT). *IEEE Trans. Antennas Propag.* **71** (10), 7980–7991. <https://doi.org/10.1109/TAP.2023.3306182> (2023).
- Lu, P., Yang, X. S., Li, J. L. & Wang, B. Z. A compact frequency reconfigurable rectenna for 5.2 and 5.8 GHz wireless power transmission. *IEEE Trans. Power Electron.* **30** (11), 6006–6010. <https://doi.org/10.1109/TPEL.2014.2379588> (2015).
- Chang, M., Li, Y., Han, J., Liu, H. & Li, L. A compact polarization-insensitive rectenna with harmonic suppression for wireless power transfer. *IEEE Antennas Wirel. Propag. Lett.* **23** (1), 119–123. <https://doi.org/10.1109/LAWP.2023.3319317> (2024).
- Liu, Y., Huang, K., Yang, Y. & Zhang, B. A low-profile lightweight circularly polarized rectenna array based on coplanar waveguide. *IEEE Antennas Wirel. Propag. Lett.* **17**, 9, 1659–1663. <https://doi.org/10.1109/LAWP.2018.2861938> (2018).
- Ha, T. D., Nie, X., Bağcı, H., Erricolo, D. & Chen, P. Y. A low-profile, wide-angle, and bandwidth-enhanced rectenna for radiative energy harvesting in the 12 GHz band. *IEEE Antennas Wirel. Propag. Lett.* **23** (11), 3807–3811. <https://doi.org/10.1109/LAWP.2024.3387925> (2024).
- Patil, D. D., Subramanian, K. S. & Pradhan, N. C. 3-D-printed dual-band rectenna system for green IoT application. *IEEE Trans. Circuits Syst. II Exp. Briefs*. **70** (8), 2864–2868. <https://doi.org/10.1109/TCSII.2023.3298367> (2023).
- Moloudian, G., Buckley, J. L. & O'Flynn, B. A novel rectenna with class-F harmonic structure for wireless power transfer. *IEEE Trans. Circuits Syst. II Exp. Briefs*. **71** (2), 617–621. <https://doi.org/10.1109/TCSII.2023.3315152> (2024).
- Shen, J. et al. A compact duplexing rectenna with wireless power transfer and harmonic feedback capabilities. *IEEE Antennas Wirel. Propag. Lett.* **22**, 7, 1751–1755 (2023).
- Shi, J. et al. A High-Efficiency, Simple-Structure, Compact Wideband Microwave Energy Harvester for Wirelessly Powered IoT Receivers. *IEEE Internet Things J.* **12**, 13, 23510–23523. <https://doi.org/10.1109/JIOT.2025.3553958> (2025).
- Zhang, X., Cao, C. & Song, C. A compact dual-band dual circular polarization wideband rectenna using reverse Wilkinson power divider for wireless information and power transfer. *IEEE Antennas Wirel. Propag. Lett.* **23**, 9, 2728–2732. <https://doi.org/10.1109/LAWP.2024.3405579> (2024).
- Ojha, S. S. et al. A dual ultra-wideband rectenna with a compact conical antenna for RF energy harvesting from S and C bands. *Results Eng.* **22**, 102279 (2024).
- Wang, M., Yang, L. & Shi, Y. A dual-port microstrip rectenna for wireless energy harvesting at LTE band. *AEU – Int. J. Electron. Commun.* **126**, 153451 (2020).
- Li, J., Li, Z., Jiang, C., Wei, T. & Liu, Z. Designing and modeling of a dual-band high-efficiency rectenna using dielectric resonant antenna array. *Appl. Sci.* **12**, 19, 10081 (2022).
- Barakat, A., Jordan, W. & Pokharel, R. K. Compact dual-band rectifier with self-matched branches using comprehensive impedance control. *Electronics* **14** (5), 933 (2025).
- Bougas, I. D. et al. Quad-band rectifier circuit design for IoT applications. *Technologies* **12** (10), 188 (2024).
- Alcaraz López, O. L. & Suto, K. RF energy harvesting and wireless power transfer for IoT. *Sensors* **24**, 7567 (2024).
- Sun, X., Zhang, J., Wang, W. & He, D. A wearable dual-band magnetoelectric dipole rectenna for radio frequency energy harvesting. *Electronics* **14**, 7, 1314 (2025).
- Ali, A. et al. Dual-band 802.11 RF energy harvesting optimization for IoT devices with improved patch antenna design and impedance matching. *Sensors* **25** (4), 1055 (2025).
- Atanasov, N., Atanasov, B. & Atanasova, G. Flexible rectenna on an eco-friendly substrate for application in next-generation IoT devices. *Appl. Sci.* **15** (11), 6303 (2025).
- Halimi, M. D. A., Al-Naib, I. & Attia, H. Multi-band microwave rectifiers for RF energy harvesting: A comprehensive review of design techniques and performance analysis. *IEEE Access*. **13**, 140061–140078. <https://doi.org/10.1109/ACCESS.2025.3597133> (2025).
- Liu, Z. et al. Enhanced wireless power transfer system efficiency using a pattern reconfigurable antenna for mobile charging. *IEEE Antennas Wirel. Propag. Lett.* **24**, 11, 4242–4246. <https://doi.org/10.1109/LAWP.2025.3589749> (2025).
- Chandrasekaran, K. T. et al. Compact dual-band metamaterial-based high-efficiency rectenna for ambient electromagnetic energy harvesting. *IEEE Antennas Propag. Mag.* **62** (3), 18–29. <https://doi.org/10.1109/MAP.2020.2982091> (2020).
- Nosrati, M., Rezaei, P., Danaie, M. & Khalilpour, J. Broadband compact rectenna system using a Wilkinson power divider to harvest microwave energy. *Sci. Rep.* **15** (17717). <https://doi.org/10.1038/s41598-025-02555-1> (2025).
- Hamed, A. R. & Al-Absi, M. A. Co-Design of Silicon-Based CMOS Rectifiers and Impedance Matching Networks for Low-Power IoT Systems: Trends and Insights. *IEEE Access*. **13**, 183855–183885. <https://doi.org/10.1109/ACCESS.2025.3624823> (2025).

29. Halimi, M. A., Khan, T., Kishk, A. A. & Antar, Y. M. M. Efficient rectifier circuit operating at N78 and N79 sub-6 GHz 5G bands for microwave energy-harvesting and power transfer applications. *Int. J. Microw. Wirel. Technol.* **16** (1), 75–82 (2024).
30. Meher, P. R., Mishra, S. K. & Halimi, M. A. A Low-Profile Compact Broadband CP DRA for RF Energy Harvesting Applications. *IETE J. Res.* **70** (5), 4540–4548. <https://doi.org/10.1080/03772063.2023.2237469> (2024).

### Acknowledgements

This research was financially supported by Princess Nourah bint Abdulrahman University Researchers Supporting Project number (PNURSP2026R235), Princess Nourah bint Abdulrahman University, Riyadh, Saudi Arabia.

### Author contributions

Author Contributions: All authors have contributed to the article to be recognized as co-authors of this article. Conceptualization, Methodology: H.B.H; Implementation: A.A.R and S.G; Draft Preparation: M.S.K; Supervision: R.G; Writing, Reviews: N.B; Editing: A.G; Writing, Reviews, and Editing: L.B.

### Funding

This research was financially supported by Princess Nourah bint Abdulrahman University Researchers Supporting Project number (PNURSP2026R235), Princess Nourah bint Abdulrahman University, Riyadh, Saudi Arabia.

### Declarations

#### Competing interests

The authors declare no competing interests.

#### Additional information

**Correspondence** and requests for materials should be addressed to L.B.

**Reprints and permissions information** is available at [www.nature.com/reprints](http://www.nature.com/reprints).

**Publisher's note** Springer Nature remains neutral with regard to jurisdictional claims in published maps and institutional affiliations.

**Open Access** This article is licensed under a Creative Commons Attribution-NonCommercial-NoDerivatives 4.0 International License, which permits any non-commercial use, sharing, distribution and reproduction in any medium or format, as long as you give appropriate credit to the original author(s) and the source, provide a link to the Creative Commons licence, and indicate if you modified the licensed material. You do not have permission under this licence to share adapted material derived from this article or parts of it. The images or other third party material in this article are included in the article's Creative Commons licence, unless indicated otherwise in a credit line to the material. If material is not included in the article's Creative Commons licence and your intended use is not permitted by statutory regulation or exceeds the permitted use, you will need to obtain permission directly from the copyright holder. To view a copy of this licence, visit <http://creativecommons.org/licenses/by-nc-nd/4.0/>.

© The Author(s) 2026